Available online at www.elixirpublishers.com (Elixir International Journal)

Condensed Matter Physics

Elixir Condensed Matter Phys. 60 (2013) 16407-16419

Elixir ISSN: 2229-712X

Interband absorption coefficients in a strained $Zn_{0.2}Cd_{0.8}S/ZnS$ quantum dot

A.Azhagu Parvathi[1] and A.John Peter[2*]
[1]Department of Physics, VV Vanniaperumal College for Women, Virudhunagar-626 001.India.
[2]Department of Physics, Govt.Arts and Science College, Melur-625 106. Madurai, India.

ARTICLE INFO

Article history:
Received: 23 May 2013;
Received in revised form:
24 June 2013;
Accepted: 12 July 2013;

Keywords
Exciton binding energy,
Piezoelectricity and spontaneous polarization,
Quantum dot.

ABSTRACT

Interband optical absorption coefficients in a strained $Zn_{0.2}Cd_{0.8}S/ZnS$ quantum dot are discussed theoretically taking into account the internal field induced by the spontaneous and piezoelectric polarizations. The effects of geometrical quantum confinement on the exciton binding energies in $Zn_xCd_{1-x}S/ZnS$ quantum dot are investigated for various confinement potentials and thereby the interband optical transition energy associated with the photon is brought out. The effects of quantum confinement on the heavy hole exciton are brought out here. We calculate the oscillator strengths for the heavy hole and light hole excitons and the total nonlinear optical absorption coefficients in a $Zn_{0.2}Cd_{0.8}S$ /ZnS quantum dot with the incident photon energy taking into account the effective mass anisotropy of holes. Our results bring out that the oscillator strength depends on the geometrical confinement, electron and hole wave functions and the interaction between them, and the nonlinear optical absorption coefficient shows larger values for smaller dots.

1.Introduction

Present decade is witnessing a tremendous improvement in the study of optical and electro-optical properties in the low dimensional semiconductor systems due to the invention of novel experimental techniques. Nano-semiconductors with the desired sizes are manufactured out of these techniques. Spherical semiconductor nanocrystals with the diameter ranging between 1nm and 5nm are synthesized using some simple experimental methods such as wet chemical approach. Moreover, these low dimensional semiconductor nanostructures depend on the energy spectrum of a confined exciton in order to bring out the exotic behaviour of the physical properties with the effect of quantum confinement. These unique properties are used for biological imaging and sensing and may replace the conventional fluorophores with the multiple fluorescence emission [1]. The quantized energies as well as the motion of the exciton will lead a widening band gap if the radius of the nanocrystal smaller than the exitonic Bohr radius [2,3]. The reports in this emerging field direct us to produce novel materials involving some potential applications especially in non-linear opto-electronic devices for controlling the optical signals in optical computers [4,5].

Semiconductor nanocrystals especially II-VI compound nanoparticles will have a large number of potential applications such as photovoltaic cells and luminescent materials [6,7] due to its tunable band gap if the impurities are introduced with the appropriate proportion. The $CdS/Zn_xCd_{1-x}S$ quantum dot has a large lattice mismatch between the well and barrier layers. So it is important to include the effect of biaxial strain induced by the lattice mismatch which eliminates the degeneracy of the top of valence band. Spontaneous and piezoelectric polarizations, generating built-in electrostatic field especially in wurtzite heterostructures, determine the quantum states of excitons in a quantum dot. $Zn_xCd_{1-x}S$ is a direct band gap material, and its band gap varies with the range 2.5 eV- 3.5 eV, a promising candidate for light emitting diodes with visible emissions with the proper introduction of Cd content. Hence it becomes more important to understand the excitonic recombination and the band alignment of CdS $/Zn_xCd_{1-x}S$ compounds. A larger exciton

---

Tele: +91 9786141966
E-mail addresses: a.john.peter@gmail.com

binding energies than the thermal energy at room temperature can be applied for generating light in light emitting diodes if the excitons in the particular material are stable at the room temperature [8].

In the present work, we calculate the quantized energies of the ground state of heavy hole and light hole in a strained $Zn_xCd_{1-x}S/ZnS$ quantum dot with various Zn alloy content and thereby we have computed the interband optical transition energy. We investigate the exciton binding energies for various confinement potentials by varying Zn composition in the $Zn_xCd_{1-x}S/ZnS$ quantum dot and the interband emission energy due to heavy hole is computed. The interband transitions of $Zn_xCd_{1-x}S/ZnS$ quantum dot, for various Zn alloy content, are discussed with the geometrical confinement and the strain effect. We also study the nonlinear optical absorption as a function of photon energy for a $Zn_{0.2}Cd_{0.8}S/ZnS$ quantum dot of radius 60Å and 100Å. After the introduction in Section 1, we present the computational method followed in our model in Section 2 while the results and discussion are presented in Section 3. Conclusions are summarized in the last Section.

2. CALCULATIONS AND METHODS

Here, the $Zn_xCd_{1-x}S$ material with different Zn alloy content is taken as quantum dot inner material with ZnS as barrier material. The model consists of an electron and a hole which interact with the screened Coulomb potential. Within the framework of single band effective mass approximation, the Hamiltonian of the exciton considering a strained spherical $Zn_xCd_{1-x}S/ZnS$ quantum dot is given as,

$$\left[-\frac{\hbar^2}{2m^*_{e,h}}\frac{d^2}{dr^2_{e,h}}+V_{e,h}(r)-eFz-\frac{e^2}{\varepsilon|r_e-r_h|}\right]\psi_{e,h}(r_{e,h})=0 \tag{1}$$

where $V_{e,h}(r)$ is the strain induced confinement potential and ε is the static dielectric constant. The origin of the co-ordinate system is taken from the centre of the dot material in this problem. The band gap of the material is given by [9]

$$\Delta E_g(Zn_xCd_{1-x}S) = 2.501+0.328x+0.921x^2 \text{ (eV)} \tag{2}$$

The above expression of band gap has been obtained by varying Cd concentration in ZnS powders (Fig.(1)) by taking various concentration of Cd and thereby calculating optical energy band gap. Similar expression has been obtained by other investigators [9,10]. The quadratic term in Eq. 2 is correlated with the bowing of optical band gap [11]. This approximation directs us to distribute the band gap discontinuities between $Zn_xCd_{1-x}S$ dot and ZnS barrier as $V(r)=0.7\Delta E_g$. The confinement potentials for electrons, $V_e(r)$, and holes, $V_h(r)$, are given as

$$V_e(r)=\begin{cases}0 & r\le R\\ V_e & r>R\end{cases} \tag{3}$$

and

$$V_h(r)=\begin{cases}0 & r\le R\\ V_{hh}\quad or\quad V_{lh} & r>R\end{cases} \tag{4}$$

where V_e, V_{hh} and V_{lh} are the confinements potentials of conduction band , heavy hole and light hole band offsets taken as 1822 meV, 781 and 728 meV respectively. These values increase with x as the band gap between the inner and outer material increases.

The strain-induced potential for the conduction band can be expressed as [12]

$$V_{Cstrian}(x) = a_c(x)(\varepsilon_{xx}(x) + \varepsilon_{yy}(x) + \varepsilon_{zz}(x)) \qquad (5)$$

where a_c is the deformation potential constant of conduction band, $\varepsilon_{xx}(x) = \varepsilon_{yy}(x) = \frac{a_0(x) - a(x)}{a(x)}$ where a_0 is the equilibrium lattice constant for the strained layer and a is the unstrained lattice constant and $\varepsilon_{zz}(x) = -2\frac{C_{12}(x)}{C_{11}(x)}\varepsilon_{xx}(x)$, the values of parameters are given in Table 1.

Table 1. Material parameters* used in the calculations (linearly interpolated from the data of ZnS and CdS)

Parameter	**CdS**	**ZnS**	**$Zn_xCd_{1-x}S$**
m_e^*	0.21	0.40	0.21+0.19x
γ_1	3.158	2.721	3.158-0.437x
γ_2	0.746	0.841	0.746+0.095x
e_{31}	-0.159	-0.16	-0.159-0.0001x
e_{33}	0.347	0.21	0.347-0.137x
C_{13}(GPa)	39.4	74.6	39.4+35.19x
C_{33}(GPa)	93.8	81.7	93.8-12.09x
ε	8.9	8.5	8.9-0.4x
a_c (eV)	- 0.24	-4.09	-0.24-3.846x
a_v(eV)	0.56	2.31	0.56 +1.751
a(nm)	0.582	0.541	0.582-0.041
E_g (eV)	2.50	3.53	2.50+1.031x

*parameters taken from the Ref. [24-27]

The strain-induced potential for the valence band can then be written as [13]

$$V_{Vstrain}(x) = a_v(x)(\varepsilon_{xx}(x) + \varepsilon_{yy}(x) + \varepsilon_{zz}(x)) - \frac{b(x)}{2}(\varepsilon_{xx}(x) + \varepsilon_{yy}(x) - 2\varepsilon_{zz}(x)) \qquad (4)$$

where $a_v(x)$ and b(x) are the x dependent deformation potential constants of valence band.

The strength of the built-in electric field F caused by the spontaneous and piezoelectric polarizations in the $Zn_xCd_{1-x}S$/ZnS strained quantum dot expressed as [14]

$$F(x) = \begin{cases} \left| -\frac{P_{SP}^{CdS}(x) + P_{PE}^{CdS}(x) - P_{SP}^{Zn_xCd_{1-x}S}(x)}{\varepsilon_0 \varepsilon_e^{CdS}(x)} \right| & r < R \\ 0 & r \geq R \end{cases} \qquad (5)$$

Here, ε_e^{CdS} is the electronic dielectric constant of CdS and $P_{PE}^{CdS}, P_{SP}^{CdS}$ and $P_{SP}^{Zn_sCd1_{-x}S}$ are the piezoelectric polarizations and the spontaneous polarizations of CdS and the spontaneous polarization of $Zn_xCd_{1-x}S$, respectively.

The above values can be generally calculated by the polarity of the crystal and the strains of the quantum nanostructure. Since the wurtzite crystal lattice of CdS and ZnS lack inversion symmetry, the heterostructure will have spontaneous polarization (P^{SP}) and the piezo electric polarization (P^{PZ}) due to strain caused by the lattice mismatch between CdS and ZnS material.

The composition of Zn alloy dependent piezo electric polarization along the c-axis is given by

$$P^{PZ}(x) = e_{31}(x)(\varepsilon_{xx}(x) + \varepsilon_{yy}(x)) + e_{33}(x)\varepsilon_{zz}(x) \tag{6}$$

with $\varepsilon_{xx}(x) = \varepsilon_{yy}(x) = \dfrac{a(CdS) - a(Zn_xCd_{1-x}S)}{a(CdS)}$ and $\varepsilon_{zz}(x) = -2\dfrac{C_{13}(x)}{C_{33}(x)}\varepsilon_{xx}(x)$, the values of parameters are given in Table 1. The piezo electric polarization is given by

$$P^{PZ}(x) = 2\varepsilon_{xx}(x)\left(e_{31}(x) - \varepsilon_{33}(x)\frac{C_{13}(x)}{C_{33}(x)}\right). \tag{7}$$

Thus the total polarization is given by

$$\vec{P}(x) = \vec{P}^{PZ}(x) + \vec{P}^{SP}(x). \tag{8}$$

The electron effective mass m_j^* is given by

$$m_j^*(x) = \begin{cases} m_I^*(x) & r < R \\ m_{II}^*(x) & r \geq R \end{cases} \tag{9}$$

$m_I^*(x)$ and $m_{II}^*(x)$ denote the x dependent reduced effective mass of the inside and outside the quantum dot. The material parameters are given in Table.1 and Table.2.

The heavy and light hole effective masses are given by

$$\frac{1}{m_{hh}} = \frac{1}{m_0}(\gamma_1 - 2\gamma_2) \tag{10}$$

$$\frac{1}{m_{lh}} = \frac{1}{m_0}(\gamma_1 + 2\gamma_2) \tag{11}$$

where m_0 is the free electron mass. We choose a trial wave function as follows

$$\Psi(r_e, r_h) = |\psi(r_e)\rangle |\psi(r_h)\rangle \psi(r)\rangle \tag{12}$$

The ground state wave function of the electron (hole) confined in the strained $Zn_xCd_{1-x}S/ZnS$ quantum dot can be written as

$$\psi(r_j) = \frac{1}{r_j}\varphi(r_j)Y_l^m(\theta,\phi) \tag{13}$$

where $Y_l^m(\theta,\phi)$ are the complex spherical harmonics and $\varphi(r)$ is the radial wave function and the corresponding confinement energy equation of the electron (hole) can be obtained by using the *m*-order Bessel function J_m and the modified Bessel function K_m as

$$\psi(r,\theta,\varphi)=\begin{cases} N_1 e^{\pm il\phi} J_l(r_{nl}r) & r<R \\ N_1 \dfrac{J_l(r_{nl}R)}{K_l(b_{nl}R)} e^{\pm il\phi} K_l(b_{nl}r) & r\geq R \end{cases} \tag{14}$$

where N$_1$ is the normalization constant,

$$r_{nl}=\sqrt{\frac{2m_j^* E_{nlk}}{\hbar^2}}\,, \tag{15}$$

and

$$b_{nl}=\sqrt{\frac{2m_j^*(V-E_{nlk})}{\hbar^2}}\,, \tag{16}$$

where r$_{nl}$ is the nth root satisfying the equation

$$r_{nl}\frac{dJ_l(r_{nl}r)}{d(r_{nl}r)}\bigg|_{r=R} = b_{nl}\frac{J_l(r_{nl}r)}{K_l(b_{nl}r)}\frac{dK_l(b_{nl}r)}{d(b_{nl}r)}\bigg|_{r=R}, \tag{17}$$

And E$_{nlk}$ is the lowest binding energy calculated by solving the transcendental equation

$$\sqrt{E}J_1(\sqrt{E}R)K_0(\sqrt{(V-E)}R)=(\sqrt{(V-E)}K_1(\sqrt{(V-E)}R)J_0(\sqrt{E}R)\,, \tag{18}$$

This fixes the values of r$_{nl}$ and b$_{nl}$ for the lowest values of E$_{nlk}$ after matching the wave functions and their derivatives at boundaries of the quantum dot along with the normalization.

The variation trial wave function $|\psi(r)\rangle$ describing the internal motion between the electron and the hole in the system, taken to be the lowest state of the exciton energy is given by

$$|\psi(r)\rangle=\exp(-\alpha r^2) \tag{19}$$

where α is the variational parameter. We calculate the ground state energy E_{exc} by finding out the expectation value of the energy of the Hamiltonian, Eq.(1), as

$$\langle E_{exc}\rangle=\min_{\alpha}\frac{\langle\psi_{r_e}|H_{exc}|\psi_{r_e}\rangle}{\langle\psi_{r_e}|\psi_{r_e}\rangle} \tag{20}$$

The exciton binding energy is calculated as

$$E_b=E_e+E_h-E_{exc} \tag{21}$$

And the optical transition energy is computed by subtracting the heavy-hole exciton binding energy from the effective heavy-hole bandgap energy and the lowest binding energies of electron and hole. Thus, the interband emission energy E$_{ph}$ associated with the exciton is calculated using the following equation

$$E_{ph}=E_e+E_h+E_g-E_{exc} \tag{22}$$

where E$_e$ and E$_h$ are the confinement energies of electron and hole respectively. E$_g$ is the band gap energy of CdZnS material.

For the excited states, the Eq.(1) may be written as

$$\left[-\frac{\hbar^2}{2m^*_{e,h}}\frac{d^2}{dr^2_{e,h}}+V_{e,h}(r)+\frac{l_{e,h}(l_{e,h}+1)\hbar^2}{2m^*_{e,h}r^2_{e,h}}-eFz-\frac{e^2}{\varepsilon|r_e-r_h|}\right]\psi_{e,h}(r_{e,h})=0 \qquad (23)$$

where l denotes the quantum numbers associated with the operator **L**. The wave function $\varphi(r)$ is considered to be zero at the centre of the nanosphere. For the excited states, $l \neq 0$, Eq.(23) may be solved by using the Bessel functions as an orthonormal basis set as done earlier.

The dipole transition matrix element between the initial state and final state is given by

$$\langle M_z\rangle_{fi}=e\left\{\int_0^R(\varphi_f^{r<R})^*r\cos\theta\varphi_i^{r<R}d\tau+\int_R^\infty(\varphi_f^{r>R})^*r\cos\theta\varphi_i^{r>R}d\tau\right\} \qquad (24)$$

For any electronic system transitions, these calculations are imperative to compute the different optical properties. However, the dipole transition transitions are allowed using the selection rules $\Delta l=\pm 1$ where l is the angular momentum quantum number. In addition to that the oscillator strength which is related to the dipole transition, expressed as

$$P_{fi}=\frac{2m^*}{\hbar^2}\Delta E_{fi}|M_{fi}|^2 \qquad (25)$$

where $\Delta E_{fi}=E_f-E_i$ refers the difference of the energy between the lower and upper states. $M_{fi}=2\langle f|\vec{R}|i\rangle$ is the electric dipole moment of the transition from i state to f state in the quantum dot. The observation of oscillator strength is imperative especially in the study of optical properties and they are related to the electronic dipole allowed absorptions. Moreover, the outcome of the results will viewed on the fine structure of the optical absorption.

The Schrödinger equation is solved variationally by finding $\langle H\rangle_{\min}$ and the binding energy of the exciton in the spherical quantum dot is given by the difference between the energy with and without Coulomb term. First, we concentrate on the calculation of the electronic structure of the $Zn_xCd_{1-x}S/ZnS$ quantum dot system by calculating its subband energy (E) and subsequently the exciton binding energy. Then, by using the density matrix approach, within a two-level system approach, the explicit expression for the optical absorption is computed in saturation limit.

The linear optical absorption coefficient is given by [16]

$$\alpha^1(\omega)=2\pi\omega\sqrt{\frac{\mu_0}{\varepsilon_r}}\frac{\rho e^e|M_{fi}|^2\hbar\tau_{12}}{(\hbar\omega-E_{21})^2+(\hbar\tau_{12})^2} \qquad (26)$$

and the third order nonlinear optical absorption coefficient is expresses as

$$\alpha^3(\omega)=-2\pi\omega\sqrt{\frac{\mu_0}{\varepsilon_r}\left(\frac{1}{2\varepsilon_0 n_r c}\right)}\frac{\rho e^4|M_{fi}|^2\hbar\tau_{21}}{\left[(\hbar\omega-E_{21})^2+(\hbar\tau_{12})^2\right]^2}\left\{\begin{matrix}4|M_{fi}|^2- \\ \dfrac{(M_{22}-M_{11})^2[3E_{21}^2-4E_{21}\hbar\omega+\hbar^2(\omega^2-\tau_{21}^2)}{E_{21}^2+(\hbar\tau_{21})^2}\end{matrix}\right\} \qquad (27)$$

where the dipole matrix element between the initial and final states as defined earlier , μ_0 is the permeability of the system, n_r is the refractive index of the dot material, ρ is electron density of the quantum dot, $\hbar\omega$ is the incident photon energy, ε_0 is the dielectric permittivity of the vacuum, $E_1(E_2)$ is the initial (final) state energy, $E_{21} = E_2 - E_1$ is the energy difference between the final and initial states, $\Gamma_{12} = 1/\tau$ is the relaxation rate for states 1 and 2 here τ is the relaxation time. ω the angular frequency of the incident photon energy, c is the speed of light in the free space, ε_0 is the electrical permittivity of the vacuum. E_1 and E_2 denote the confinement energy levels for the ground and the first excited state, respectively.

The total optical absorption coefficient is given by

$$\alpha(\omega, I) = \alpha^1(\omega, I) + \alpha^3(\omega, I) \tag{28}$$

where I is the optical intensity taken as 1MW/cm^2.

3. Results and discussion

Numerical calculations have been carried out to compute the exciton binding energy with and without inclusion of built-in internal field in the $Zn_xCd_{1-x}S$ dot over ZnS quantum barrier material with the heavy hole mass. The interband emission energies are computed as a function of dot radius for three different Zn content of the host material. Some nonlinear optical properties with the photon energy are discussed for two different dot radii in a $Zn_{0.2}Cd_{0.8}S$/ZnS quantum dot. The atomic units are used in the determination of electronic energies in which the electron charge, Planck's constant are assumed to be unit. All the values of the parameters are given in Table.1. The values with different Zn content have been obtained using linear interpolation with the available data of binary elements.

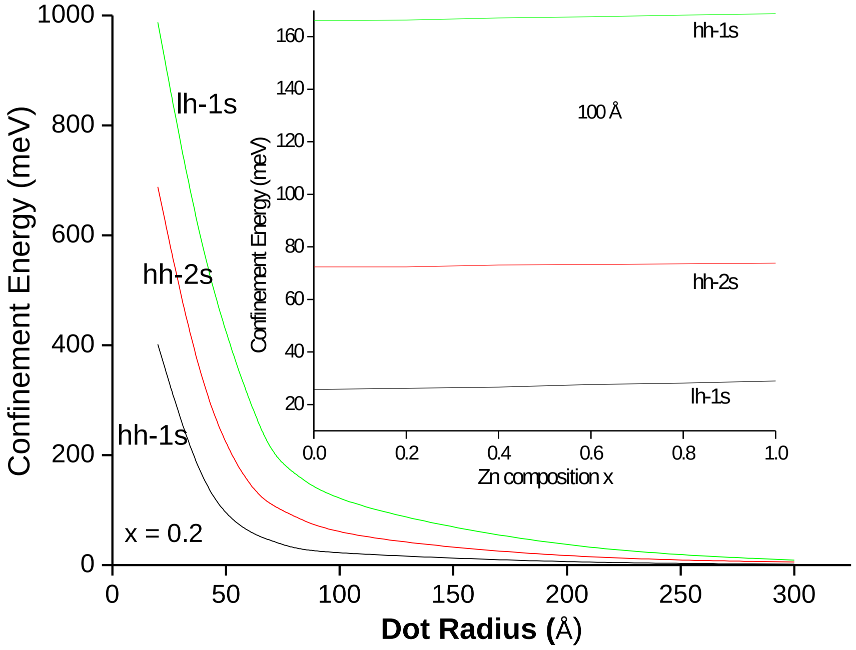

Fig.1 The subband energies of hh-1s, hh-2s and lh-1s in a $Zn_{0.2}Cd_{0.8}S$ /ZnS finite quantum dot as a function of dot radius and the insert figure shows the confinement energies of hh-1s, hh-2s and lh-1s states with the Zn composition for a 100 Å dot radius of $Zn_{0.2}Cd_{0.8}S$ /ZnS quantum dot.

Fig.1 shows the subband energies of 1s and 2s for heavy holes and 1s for light hole in a $Zn_{0.2}Cd_{0.8}S$ quantum dot as a function of dot radius and the insert figure shows the confinement energies of hh-1s, hh-2s and lh-1s states with the

Zn composition for a 100 Å dot radius of CdZnS. The lowest binding energy is calculated using Eq.(14) and the boundary condition of the heterostructure. It is inferred from the figure that the confined energies of electronic levels increase as the dot radius is decreased due to the spatial confinement. When the dot radius is large the confined electronic energies approach a value equal to the energy of the free space hydrogen. The electron confinement energy shows a significant increase with the Zn molar fraction. It is also observed that the subbands energies shift up as Zn incorporation increases adding from CdS to ZnS.

Fig.2 presents the transition energies of e-hh states and e-lh states as a function of dot radius for x = 0.2. It is seen form the figure that the transition energies increase when the dot radius of $Zn_xCd_{1-x}S$ quantum dot is decreased in all the cases. The variation of transition energies has more influence for smaller dots. It is noted that energy difference between e- hh and e-lh is particularly higher for Zn in corporation ranging from 0.2 to 1.0. The resemblance of this observation agrees with the earlier investigation [17] in which an increase of the conduction barrier height for higher Zn composition has been reported. The trend of the lowest binding energy seems to be similar but the heavy hole exciton is found to be higher than the light hole exciton. It is because the exciton Bohr radius of the heavy-hole exciton is larger than the light-hole exciton [8]. The band of inner dot ($Zn_xCd_{1-x}S$) and splitting of heavy and light hole excitons depend on the concentration of Zn alloy content and the geometrical confinement.

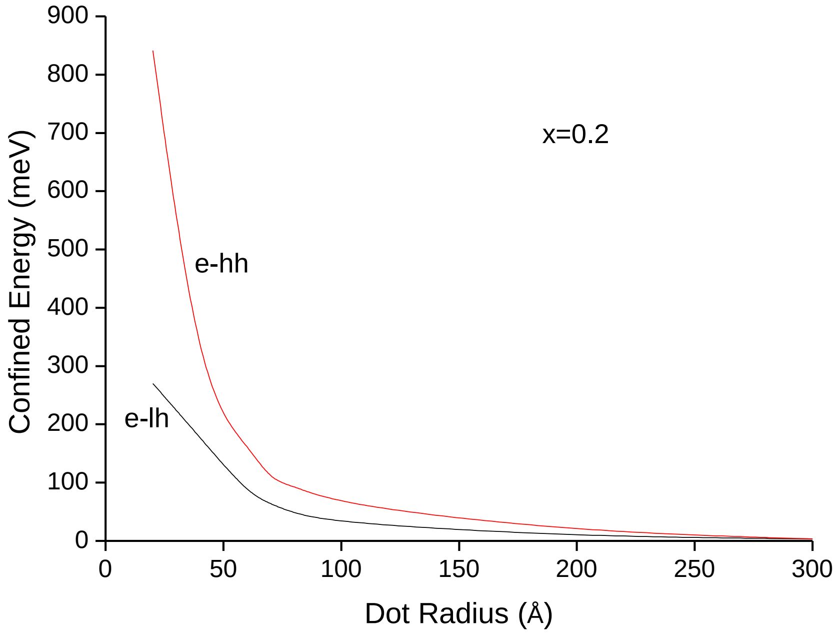

Fig.2 The transition energies of e-hh states and e-lh states as a function of dot radius in a $Zn_{0.2}Cd_{0.8}S$ /ZnS quantum dot.

Since the oscillator strength gives useful information on electronic structure and optical properties of quantum dots, we present the variation of oscillator strength for various transitions as a function of dot radius in a $Zn_xCd_{1-x}S$/ZnS quantum dot in Fig.3. The behaviour of oscillator strength of heavy and light hole excitons with the dot radius is fundamentally same. Dipole matrix element and the difference between the energies are two important parameters involved in calculating the oscillator strength. It is observed from the figure that the oscillator strength increases when the dot radius is decreased and then reaches the maximum value for all the transitions. The oscillator strength depends on the geometrical confinement, electron and hole wave functions and the interaction between them. The effect of quantum confinement on the heavy hole exciton over light hole exciton is brought out here.

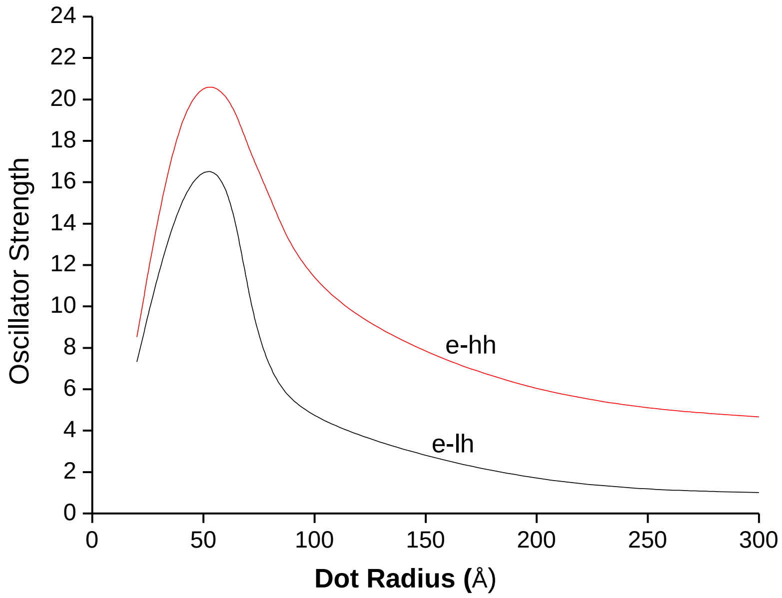

Fig.3 Variation of oscillator strength for e-hh and e-lh states as a function of dot radius in a $Zn_{0.2}Cd_{0.8}S$ /ZnS quantum dot

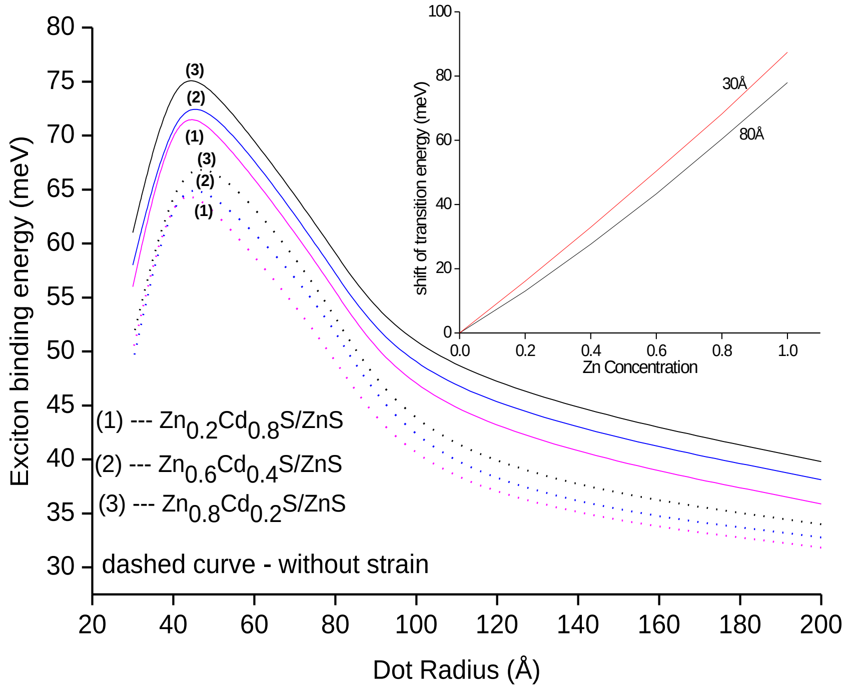

Fig.4 Variation of exciton binding energy as a function of dot radius in a $Zn_xCd_{1-x}S$/ZnS quantum dot with and without the inclusion of strain effects for three different concentration of Zn alloy content; the insert figure shows the shift in transition energy for Zn concentration for two different dot radii.

Variation of exciton binding energy as a function of dot radius of three different concentration of Zn alloy content in a $Zn_xCd_{1-x}S$/ZnS quantum dot with and without strain is shown in Fig.4 and the insert figure shows the shift in transition energy for Zn concentration for two different dot radii. The heavy hole exciton binding energy with without the strain effect is computed in order to observe the quantum confinement effects. In all the cases, the exciton binding energy increases with a decrease of dot radius, reaching a maximum value and then decreases when the dot radius still decreases. The Coulomb interaction between the electron and hole is increased which ultimately causes the decrease in binding energy when the dot radius decreases. As the dot radius approaches strong confinement the tunnelling effect dominates, the wave function squeezes out in the barrier material and this effect reduces the exciton binding energy. From the insert figure, we find the binding energy increases with the Zn alloy content as the barrier height increases as Zn alloy content increases. Further, we find that the exciton binding energy is higher when the dot radius becomes smaller due to the confinement. Further, we observe that the band gap increases as the Zn alloy content increases and it can be estimated by the expression Eq.(2). Red shift in emission energy is observed while including the strain effect induced by the spontaneous and piezoelectric effect.

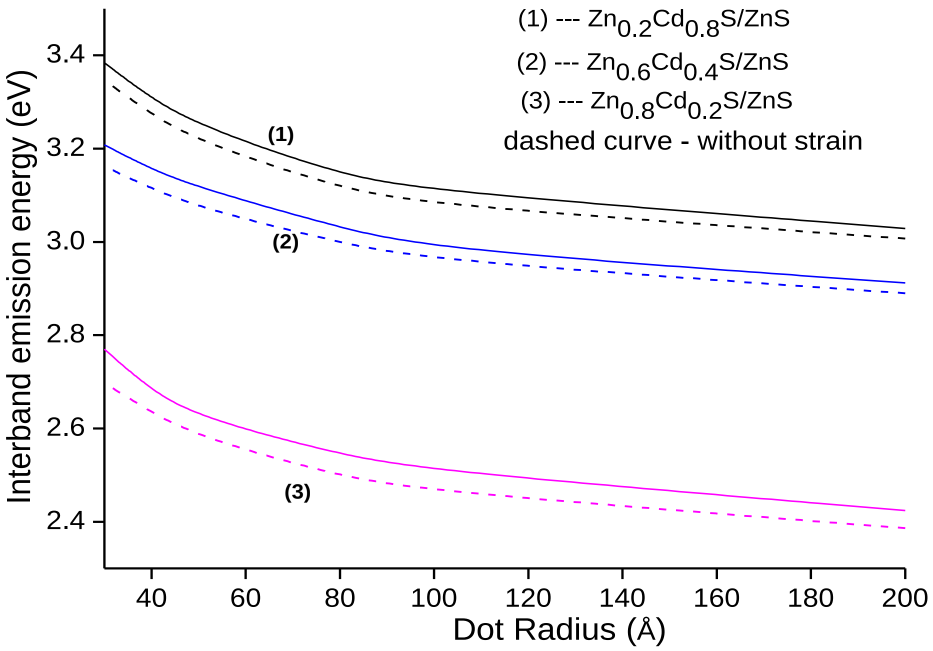

Fig.5 Variation of interband emission energy due to heavy hole as a function of dot radius in a $Zn_xCd_{1-x}S$/ CdS quantum dot with different content of Zn with and without strain.

In Fig.5, we present the variation of optical band gap as a function of dot radius of $Zn_xCd_{1-x}S$/ZnS quantum dot with different content of Cd. It is observed that the interband emission energy increases as the dot radius is decreased. This is due to the confinement of electron-hole when the dot radius is increased. Also it is observed that as concentration of Zn increases the optical band gap increases due to the enhancement of barrier height. Moreover it is clearly shown that the effect of bound exciton has influence on the interband emission energy. This representation clearly brings out the quantum size effect. We observe 2.77 eV, interband emission energy for 30 Å $Cd_{0.2}$ $Zn_{0.8}S$/ZnS quantum dot with the inclusion of strain effect. This value resembles with the interband emission energy of 2.61 eV for 25 Å $Cd_{0.2}Zn_{0.8}S$

quantum dot observed by Kunets [18]. It is also observed that the exciton transition energy lowers for all the quantum dot sizes if the strain effect due to the built-in electrostatic field is included, it is due to the decrease in the conduction band energy with the inclusion of biaxial strain. So it is important to include the stain influence of spontaneous and piezoelectric polarization. This result closely agrees with the previous investigator [19].

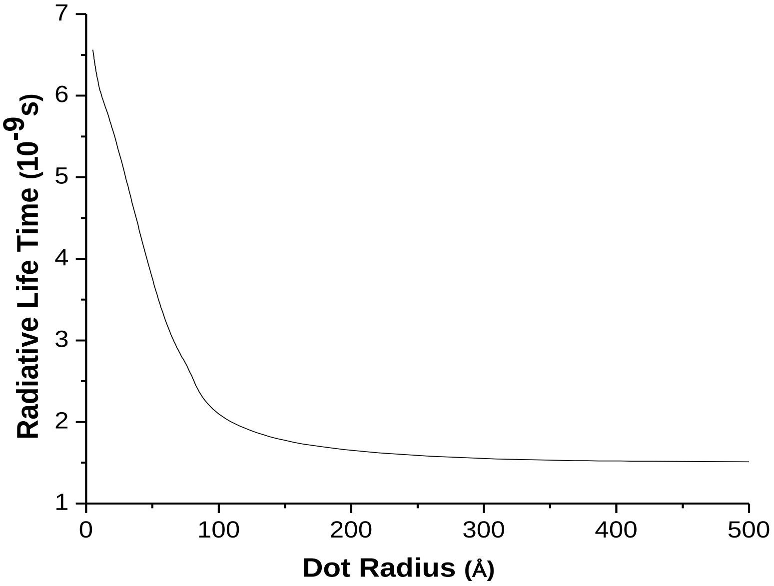

Fig.6 Exciton radiative life time of a confined heavy hole exciton as a function of dot radius in a $Zn_{0.2}Cd_{0.8}S$ /ZnS quantum dot.

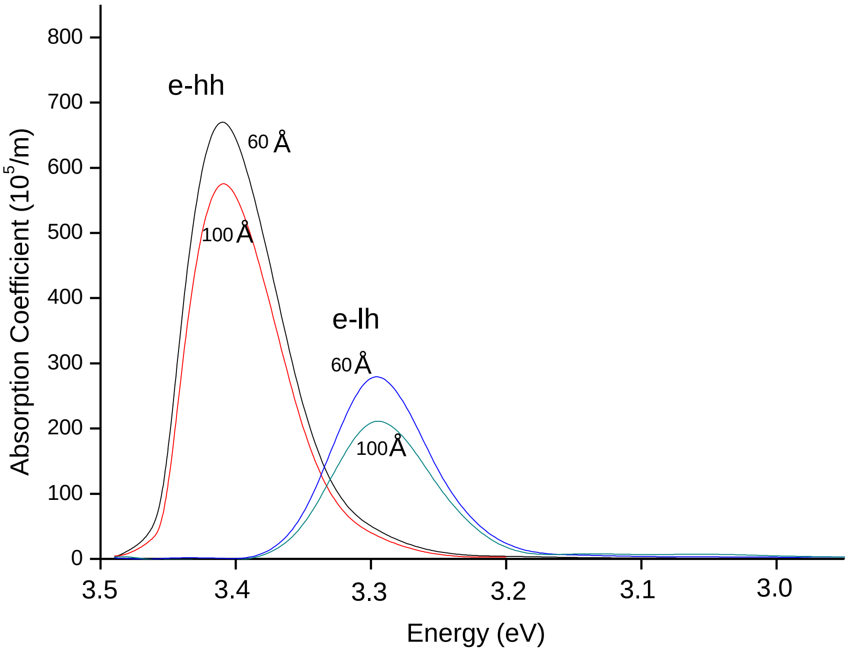

Fig.7 Variation of absorption coefficients for e-hh and e-lh states for two different dot radii (60Å and 100 Å) as a function of photon energy in a $Zn_{0.2}Cd_{0.8}S$ /ZnS quantum dot.

We display the radiative life time of a confined exciton as a function of dot radius for $Zn_{0.2}Cd_{0.8}S/ZnS$ in Fig.6. In any absorption spectra, the intensity of an exciton binding energy and the envelope wave function is characterized by the oscillator strength. The radiative life time can be calculated as [20,21]

$$\tau = \frac{2\pi\varepsilon_0 m_0 c^3 h^2}{\sqrt{\varepsilon} e^2 E_{exc}^2 f} \qquad (29)$$

where f is the oscillator strength, E_{exc} is the exciton binding energy and all the other parameters are universal physical constants. It is found that the radiative life time of exciton decreases with the dot radius. The values of radiative life time are almost constant beyond the dot radius 100Å. The results are in good agreement with the recent investigations reported by Mohanta et al., [22] who have calculated the radiative life time of $Cd_{0.25}Zn_{0.75}S$ nanocrystals as 1.64 ns and Wang et al.,[23] too have reported the same values.

Fig.7 displays the variation of linear optical absorption coefficients for heavy hole and light hole states for two different dot radii (60Å and 100 Å) as a function of incident photon energy for $Zn_{0.2}Cd_{0.8}S/ZnS$ quantum dot. It is inferred from the figure that the maximum absorption coefficient occurs at the corresponding value of the threshold photon energy ($E_{fi} = \hbar\omega$) in all the two cases. The energy which is higher denotes the 1s exciton associated with the highest heavy hole valence band whereas the lower peak energy refers light hole band. The trend of this absorption coefficient for 77Å $Cd_{0.25}Zn_{0.75}S$ nanocrystals [22] exactly coincides with our results. We notice that the nonlinear optical absorption coefficient shows larger values for smaller dots than for larger dots due to the confinement. Further, it shows the stronger behaviour for smaller quantum dots since the absorption spectrum depends on the quantum dot volume. We also notice that the electronic dipolar transition matrix elements are found to be high for the transitions between the higher levels of the intensity of the total absorption coefficient which increases for the transitions between higher excited levels.

In conclusion, we have calculated the exciton binding energies and the interband emission energy in the strained $Zn_xCd_{1-x}S/ZnS$ quantum dot for different barrier heights taking into account the geometrical effects. In all our calculations, we have included the contributions of built-in strained field induced by spontaneous and piezoelectric polarizations in the $Zn_xCd_{1-x}S/ZnS$ quantum dot. The confined electron (hole) energies of ground state have been computed for various values of Zn alloy content and thereby interband transition energy has been calculated with the geometrical confinement. In all the computations, we have considered the spatial confinement on nonlinear optical properties in a $Zn_{0.2}Cd_{0.8}S/ZnS$ with the inclusion of built-in electrostatic field. The theoretical computation has been carried out using variational technique within the single band effective mass approximation. The values of the absorption edge are found to shift towards the shorter wave length region and hence the direct band gap energy varies from 2.5 eV for CdS to 3.5 eV for ZnS material. And we believe that our investigations can stimulate further research activities in device applications of Zn based CdS materials in future.

References

1. J.Ouyang, John A. Ripmeester, X.Wu, David Kingston, Kui Yu, Alan G.Joly and Wei Chen, J.Phys.Chem C 111(2007)16261.

2. B. Bhattacharjee, S.K. Mandal, K. Chakrabarti, D. Ganguli, S. Chaudhui, J. Phys. D: Appl. Phys. 35 (2002) 2636.

3. K.K. Nanda, S.N. Sarangi, S. Mohanty, S.N. Sahu, Thin Solid Films 322 (1998) 21.

4. S. I. Pokutnioe, Fiz. Tekh. Poluprovodn. (St. Petersburg) 34, 1120 (2000) [Semiconductors 34, 1079 (2000)]; J. Appl. Phys. 96 (2004) 1115.

5. C. H. Bennett and D. P. DiVincenzo, Nature 404 (2000)247.

6. M. Morkel, L. Weinhardt, B. Lohmuller, C. Heske, E. Umbach, W. Riedl, S. Zweigart, F. Karg, Appl. Phys. Lett, 97 (2001) 4482.

7. N. Karar, F. Singh, B.R. Mehta, J. Appl. Phys. 95 (2004) 656.

8. C. Onodera, J. Phys. Stud. 15/4 (2011) 4702.

9. S.Adachi, Properties of Semiconductor alloys Group-IV, III-V and II-VI Semiconductors, John Wiley & Sons Ltd.,2009

10. G.K Padam, G.L. Malhotra and S.U.M. Rao, J. Appl. Phys. 63(3) (1988) 770.

11. H.L. Hwak, J. Phs. D16 (1983) 2367.

12. R.Eason, Pulsed laser deposition of thin films. Wiley, New Jersey 2007.

13. G. L. Bir and E. Pikus, Symmetry and Strain-Induced Effects in Semiconductors, Wiley New York, 1974.

14 S. L. Chuang, Physics of optoelectronic devices, John Wiley & Sons, New York, 1995.

15. J. J. Shi and Z. Z. Gan, J. Appl. Phys. 94 (2003) 407.

16. E.M.Goldys, J.J.Shi, Physica Status Solidi B, 210 (1998)237.

17. N. Safta, A. Sakly, H. Mejri, and Y. Bouazra, Euro. Phys. J. B, 51(2006)75.

18. V.P. Kunets Semiconductor Physics, Quantum Electronics, & Optoelectronics, 2/4, 23 (1999).

19. T. Koga, J. Nitta, H. Takayanagi, and S. Datta, Phys. Rev. Lett. 88 (2002) 126601.

20. L. Cao, Y. Miao, Z. Zhang, S. Xie and G. Yang, J. Chem. Phys. 123 (2005) 024702.

21. S. I. Pokutnii, Semiconductors 44 (2010) 488.

22. D. Mohanta, S. S. Narayanan, S. K. Pal, A. K. Raychaudhuri, J. Expt. Nanosci,4 (2009) 177.

23. X. Wang, L. Qu, J. Zhang, X. Peng, and M. Xiao,, Nano Lett. 3 (2003) 1103.

24. B. Srinivasa Rao and H. S. Paul, Applied Scientific Research, 20/1 (1969) 251.

25. T. V. Anil, C. S. Menon, K. P. Jayachandran and K. Shree Krishna Kumar, Journal of Materials Science, 41/ 23 (2006) 8013.

26. S. Ben Afia, H. Belmabrouk, Thin Solid Films 516 (2008) 1608.

27. J.J.Sharkey, A.John Peter and CW Lee, IEEE, Quantum Electronics 47/11(2011) 1451.